Prediction Error Applied to Hybrid Electric Vehicle Optimal Fuel Economy

Zachary D. Asher, David A. Baker, and Thomas H. Bradley

***Abstract*—Fuel economy improvements for hybrid electric vehicles using predictive optimal energy management strategies is an active subject of research. Recent developments have focused on real-time prediction based control strategies despite the lack of research demonstrating the aspects of prediction that are most important for fuel economy improvements. In this research, driving-derived non-stochastic prediction errors are applied to a globally optimal control strategy implemented on a validated model of a 2010 Toyota Prius and the fuel economy results are reported for each type of prediction error. This article outlines first the real world drive cycle development, then the baseline model development that simulates a 2010 Toyota Prius, followed by an implementation of dynamic programming to derive the globally optimal control, and finally the use of the dynamic programming solution to evaluate prediction errors. Fuel economy comparisons are reported for perfect prediction, prediction errors from 14 alternate drive cycles, and prediction errors from 6 alternate vehicle parameters. The results show that fuel economy improvements from a globally optimal energy management strategy are maintained under mispredicted stops, traffic, and vehicle parameters, while route changes and compounded drive cycle mispredictions may result in fuel economy improvements being lost. Taken together, these results demonstrate that fuel economy improvements through predictive optimal energy management strategies can result in a reliable fuel economy improvement.**

***Index Terms*—Hybrid Electric, Vehicle, Fuel Economy, Prediction, Error, Disturbance, Energy Management, Optimal Control, Dynamic Programming, Modeling**

I. Introduction

MODERN plug-in hybrid electric vehicle (PHEV) and hybrid electric vehicle (HEV) fuel economy (FE) can be optimized for a fixed drive cycle using a vehicle predictive Optimal Energy Management Strategy (Optimal EMS).

A. What Enables an Optimal EMS: Modern Vehicles

Modern vehicles are incrementally incorporating autonomous technologies and transitioning to intelligent vehicles. An intelligent vehicle is defined as a system that can sense the driving environment and provide information or vehicle control to assist the driver in improved vehicle operation [1]. Intelligent vehicle aspects include the ability to:

- Sense the vehicle's own status and its environment [2]
- Communicate with the environment [2]
- Plan and execute the most appropriate maneuvers [1]

As modern vehicles continue to evolve into intelligent vehicles, controls can utilize this new environmental information in addition to inputs from the human driver.

Along with the evolution of modern vehicles into intelligent vehicles, conventional vehicles are being subverted by PHEVs and HEVs [3] which provide more degrees of freedom for powertrain operation. As an example, HEVs can be powered by either stored electric energy from the battery, or mechanical energy from the engine. This increase in powertrain degrees of freedom provides energy management capabilities such as regenerating energy during braking and storing excess energy from the engine during coasting [4].

B. Why an Optimal EMS is Important: Fuel Economy

Worldwide, transportation is the second largest consumer of energy behind only the industrial sector. Transportation accounts for 30% of the world's energy consumption and the transportation energy demand is projected to increase 30% by 2040 [5]. Additionally, energy consumption by combustion engine powered vehicles has the following negative impacts:

- Requires policy costs for oil importation [6] and to prevent supply disruptions [7]
- Results in the release of greenhouse gas emissions which are responsible for climate change [8]
- Results in the release of air pollution [9] which is the fourth leading cause of premature death worldwide [10]

Increases in vehicle FE reduces energy consumption, oil importation, greenhouse gas emission, and air pollution. It has been shown that implementing FE standards, labels, and policies has improved the development of fuel saving technologies which have helped combat these issues [11]. But, although FE has been steadily increasing, there is still a lot of fuel economy that can be gained.

C. Optimal EMS Background

An HEV Optimal EMS is an application of optimal control. A mathematical optimization problem is formulated by defining the mass of fuel used as a cost to be minimized over a fixed drive cycle. The result from the mathematical optimization scheme is the minimum fuel control strategy that can be used for the fixed drive cycle. The mathematical optimization problem can be implemented using either instantaneous information or with prediction information from

Manuscript received May 25, 2017. This work was supported in part by direct funding from the Gasoline Hybrid Research Group at Toyota Motor Engineering & Manufacturing North America Inc.

Zachary D. Asher is a PhD candidate, David A. Baker is a MS student, and Dr. Thomas H. Bradley is an Associate Professor in the Department of Mechanical Engineering at Colorado State University, Fort Collins, CO 80524 USA. The corresponding author is T. Bradley (email: Thomas.Bradley@ColoState.edu).

a drive cycle. But, a consistent globally optimal control is achieved with drive cycle prediction.

1) Instantaneous Optimal EMS

An instantaneous Optimal EMS is derived by finding the optimal control strategy that minimizes fuel consumption for the instant in time for which sampled data is available. For HEVs, large FE improvements can be achieved by restricting engine operation to minimum fuel consumption solution (also known as the ideal operating line [12]) which is the primary fuel saving technique employed by current HEVs [13]. In PHEVs, studies using an instantaneous Optimal EMS have led to the "charge-depleting, charge-sustaining" EMS, where all excess battery power is used first, afterwhich the battery charge is sustained [14]. Research in instantaneous optimal energy management is an active topic of research with efforts focusing on a realization of the minimal fuel consumption through instantaneous equivalence calculations between electrical energy and fuel energy [15].

2) Predictive Optimal EMS

A predictive Optimal EMS seeks to find and achieve the absolute minimum fuel consumption in the full drive cycle by enforcing global optimal control at every point. The solutions require prediction of the full drive cycle because energy trade-offs occur between all points in the drive cycle.

There have been hundreds of papers written on predictive optimal energy management over the last ten years [16], most of which describe predictive Optimal EMS that are either: derived to be the global optimal FE, derived for practical/real-time implementation, or derived based on stochastic or random drive cycle predictions. Global optimal FE derivation strategies are developed through either dynamic programming (DP) [17] or through Pontryagin's minimization principle which is based on calculus of variations [18]. For global minimum derivation strategies, DP has been the overwhelming favorite of researchers due to its ease of use, robustness, and that no derivatives or analytic expressions are required [16]. Globally optimal control strategies are difficult to implement in practice because of the large number of computations that are required. Practical implementation derivation strategies are used in applications where researchers are willing to forgo the guarantee of global optimal FE in favor of computationally efficient algorithms that can be used in current and near future vehicles. Practical implementation derivation strategies in current vehicles include optimized rules based control [19], equivalent consumption minimization strategy [20], and model predictive control [21]. Lastly, stochastic derivation strategies also forgo a guarantee of global optimal FE in favor of a robustness to stochastic prediction errors. Stochastic derivation strategies include stochastic dynamic programming [22] and adaptive equivalent consumptions minimization strategy [23].

3) Prediction Error

Prediction errors applied to a predictive Optimal EMS is theorized to have a large impact [24] but has not been adequately studied [3], [16]. There are five relevant studies that include some aspect of prediction error on a HEV Optimal EMS. But, none of these studies are strictly focused on general results regarding fuel economy from prediction errors applied to an Optimal EMS.

An early study considered the "cost of being wrong" when comparing a prediction-based Optimal EMS to charge-sustaining/charge-depleting EMS for PHEVs. They concluded that if the vehicle distance is less than predicted for the Optimal EMS, there is a significant FE loss [25]. This study suggests that prediction of the drive cycle length is important for an Optimal EMS in a PHEV, but no further conclusions can be drawn.

Another study used two stochastic Optimal EMS and applied one prediction error of a different drive cycle. It was demonstrated that FE results are approximately equivalent but no baseline FE results are shown [26]. This study has limited misprediction scope and because no baseline FE results are shown, there is no way to know if these strategies are better than a modern vehicle EMS.

Another group of researchers continued the use of a stochastic Optimal EMS and applied various levels of stochastic prediction error. They show that FE is degraded by stochastic mispredictions but are unable to find a correlation with the mean absolute percent error [27]. This study has limited applicability because it only uses stochastic prediction errors applied to a stochastic Optimal EMS.

A later study again uses a stochastic Optimal EMS but these researchers test their Optimal EMS against a large number of real world drive cycles. They were able to demonstrate FE improvements over the baseline EMS even when subject to drive cycle variations [28]. This is the most comprehensive study to date but it is only applicable to a stochastic Optimal EMS and there is no focus on the FE results from a globally Optimal EMS.

The last prediction error study investigated a real time implementable Optimal EMS subject to stochastic mispredictions. They computed the FE results for two different values of mean absolute deviation percentage and showed that FE improvements are lost at 6% mean absolute deviation percentage [29]. This study is limited in that only two mispredictions are analyzed and that the mispredictions are both stochastic.

A study that is often cited as providing insight about the aspects of prediction that are most important for an Optimal EMS needs mention. These researchers included various levels of prediction to determine a parameter for a predictive Optimal EMS [24], but their approach is strictly applicable to their chosen Optimal EMS. Additionally their study uses various levels of prediction information rather than investigating prediction error.

This research is unique in that it focuses on the effect of driving-derived prediction errors such as a mispredicted stopping event or an excess vehicle mass subjected to a globally Optimal EMS. This research is intended to aid researchers and automotive industry professionals that are seeking to develop and implement a prediction-based Optimal EMS for FE improvements.

D. Research Novel Contributions

This research makes the following novel contributions to the HEV Optimal EMS body of knowledge: (1) dynamic

programming is used to evaluate mispredictions, (2) driving-derived mispredictions are analyzed, (3) vehicle parameter mispredictions are analyzed, and (4) the dynamic programming solution matrix time state variable is converted to a distance state variable for improved misprediction robustness.

E. Organization of this paper

There are four important concepts that compose the methods of this research: expected and mispredicted drive cycle development (study 1), a validated vehicle model with expected and mispredicted parameters (study 2), the Optimal EMS derivation, and prediction error handling. Study 1 focuses on the FE impact of driving-derived velocity prediction errors, while study 2 focuses on the FE impact of real world vehicle parameter prediction errors. The FE results are compared using baseline control, perfect prediction optimal control, and mispredicted optimal control for every type of misprediction from study 1 and study 2. Relevant vehicle parameters for discussion are included and a comprehensive report of all vehicle parameters is included with this article as supplementary material.

II. Methods

To investigate the FE results from a predictive Optimal EMS, we define: drive cycle(s), the vehicle model, and the Optimal EMS. To analyze the FE results from prediction errors requires the addition of two more definitions: prediction error type and prediction error handling in the Optimal EMS.

A. Drive Cycle Development

To study the effect of driving-derived velocity prediction errors (study 1), an expected drive cycle was developed along with 14 drive cycles to serve as mispredictions.

1) The Expected Drive Cycle

To analyze the desired aspects of the Optimal EMS, a custom drive cycle with a second-by-second velocity trace is required that concentrates the features of interest into a short drive cycle. The required drive cycle features are:

- Short in length
- Urban driving conditions
- Capability to modify for multiple driving variations

A drive cycle which meets all of these criteria was chosen that starts from a parking lot in south Fort Collins, Colorado and ends at a Colorado State University research facility. A map of this drive cycle is shown in figure 1a and the associated velocity trace is shown in figure 1b.

2) Study 1: Mispredicted Drive Cycles

Study 1 focuses on vehicle velocity mispredictions which originate from driving-derived prediction errors along the route shown in figure 1, such as excess traffic or a sudden stopping event. Four different types of mispredicted drive cycles were chosen: mispredicted stops (3 cases), mispredicted route changes (3 cases), mispredicted traffic levels (4 cases), and a compounded misprediction composed of all other types of

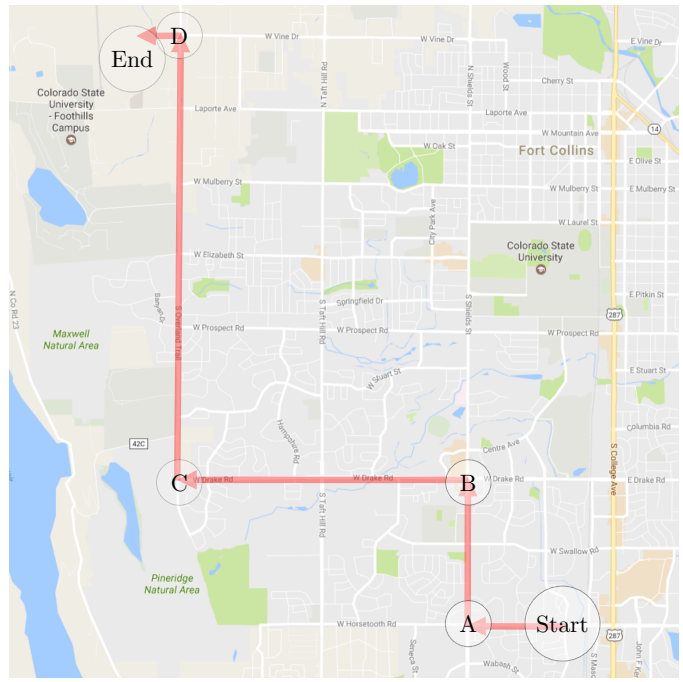

(a)

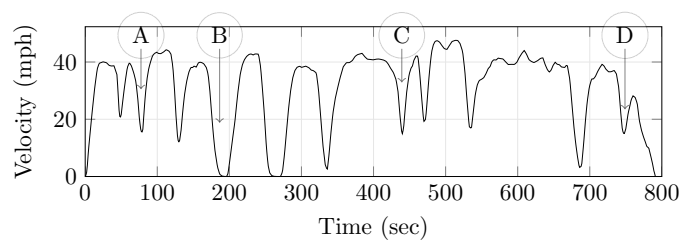

(b)

Fig. 1: The 6.9 mile chosen drive cycle in Fort Collins, Colorado as shown from a Google Maps image (a) and a velocity trace (b).

mispredictions (4 cases). To isolate the mispredictions of stops, route changes, and traffic, the velocity trace was artificially modified so that only these mispredictions would exist in the drive cycle and ensuring the drive cycle preserves its overall distance. For the cases of compounded mispredictions, real driving data was recorded while driving the same route.

The stopping event mispredictions include 1, 2, or 3 mispredicted decelerations, pauses, and accelerations associated with having not predicted a stopping event such as a pedestrian in a crosswalk or a road obstruction. The route change mispredictions abruptly end the drive cycle at three different times. The traffic mispredictions adjust the velocity trace by a factor of 1.15, 0.85, 0.75, and 0.65 for the first 335 seconds of the 791 second drive cycle while maintaining equivalent drive cycle distance. For compounded mispredictions, there are differing levels of traffic along the drive cycle, different stoplight statuses, and one of the cases includes a wrong turn. Each of the drive cycle mispredictions is shown in figure 2.

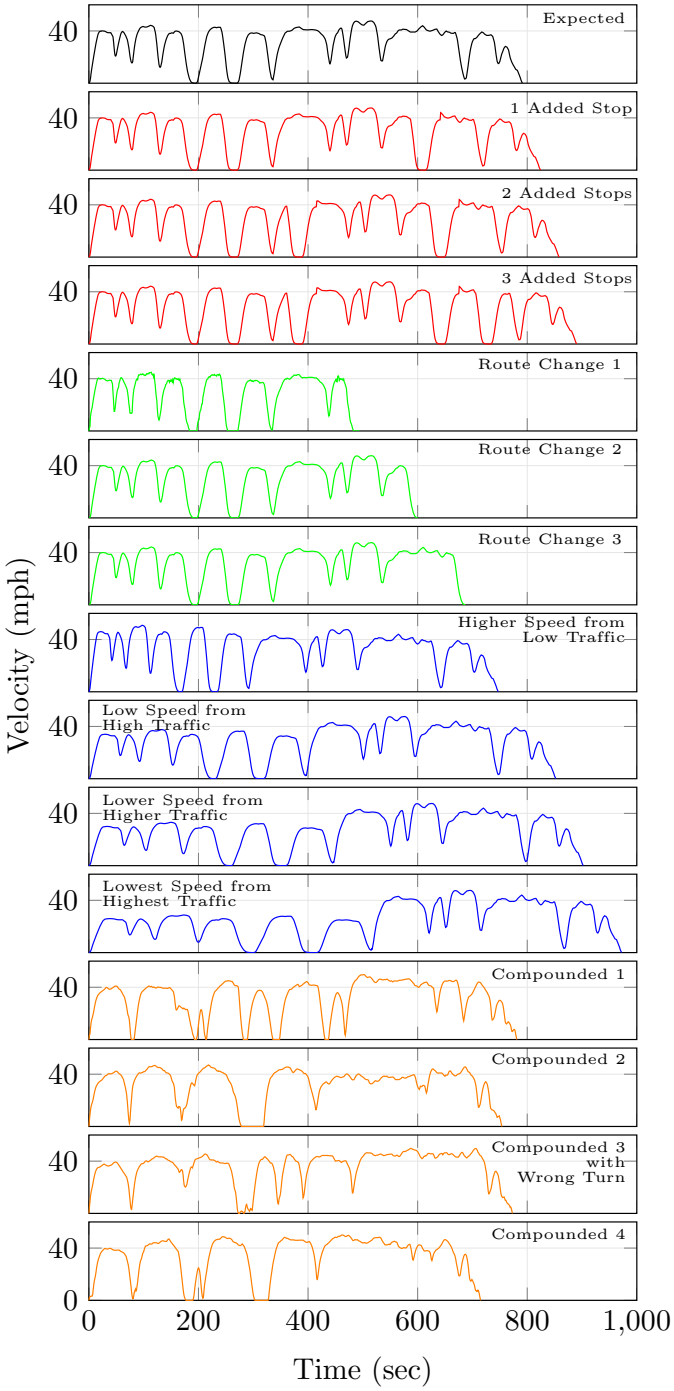

Fig. 2: All of the drive cycles used for study 1.

B. Vehicle Model: 2010 Toyota Prius

The Toyota Prius is state of the art HEV technology and it was the first modern HEV [30]; even today it still has better FE than any other vehicle in its class [31]. Because of these reasons, a 2010 Toyota Prius is an ideal vehicle to demonstrate the potential FE improvements of the Optimal EMS.

To create the model of a 2010 Toyota Prius, the publicly available parameters shown in table I were used in the Autonomie vehicle modeling software.

(a) (b)

Fig. 3: Front (a) and rear (b) view of the 2010 Toyota Prius HEV simulated in studies 1 and 2.

TABLE I: Table of significant model parameters that define the 2010 Toyota Prius (EM=electric motor, BSFC=brake specific fuel consumption).

Mechanical Parameters	
Vehicle Mass	1580.87 kg
Maximum Engine Power	73 kW
Engine BSFC map (g/kW·h)	f(Engine Torque, Engine Speed) [32]
Max Generator EM Speed	10,000 rpm
Max Traction EM Speed	13,500 rpm
Coeff. of Drag	0.259
Frontal Area	2.6005 m^2
Coeff. of Rolling Resistance	0.008
Final Drive Ratio	3.543
Ring Gear Number of Teeth	78
Sun Gear Number of Teeth	30
Wheel Radius	0.317 m
Battery Parameters	
Internal Resistance, Ω	0.373 Ω
Capacity	6.5 A·h
Open Circuit Voltage	219.7 V

1) Study 2: Mispredicted Vehicle Parameters

Of the parameters shown in table I, several of them are subject to change due to daily driving scenarios. Study 2 assumes exact vehicle velocity prediction and seeks to analyze vehicle power mispredictions. The vehicle power mispredictions chosen for analysis include mass mispredictions, drag mispredictions, and rolling resistance mispredictions. The numbers used for each of the power mispredictions are shown in table II where the average vehicle power difference along the same drive cycle was calculated from the output of Autonomie as

$$\begin{aligned}&\text{Average Vehicle Power Difference} = \\ &\quad \text{Expected Parameter Average Vehicle Power} - \\ &\quad \text{Mispredicted Parameter Average Vehicle Power} \end{aligned} \tag{1}$$

Vehicle mass mispredictions could come from extra passengers, cargo, or both. As a worst case scenario, the maximum cargo specification of 825 lbs (374 kg) from the 2010 Toyota Prius manual was used [33]. To provide a contrasting case, an elimination of an equivalent mass was used as an alternate prediction error.

Vehicle drag mispredictions could come from the addition of cargo outside the vehicle (roof rack), driving with the windows down, or even from unpredicted high winds. Research in this area suggests a loaded roof rack can cause a coefficient of drag increase of 44% and a frontal area load increase of 7% [34]. These results are dependent on the car and roof rack used for testing. As a worst case, a coefficient of drag increase of 50%

and a frontal area increase of 38% was used. A similar low drag contrasting case of a coefficient of drag decrease of 50% and a frontal area of 38% was also analyzed. This low drag case also serves as a worst case prediction scenario.

Vehicle rolling resistance mispredictions could come from the over-inflated/under-inflated vehicle tires or from road conditions. A flat tire is known to cause a rolling resistance value to increase to 30 times its original value [35] and inflation pressures can cause rolling resistance changes of 50% [36]. A 100% increase in rolling resistance was analyzed as a misprediction as well as a 50% decrease.

Additional discussion in regard to changing vehicle parameters and justification for the ranges chosen can be found in the literature [37]. Note that these researchers identified these parameter mispredictions as being important to an Optimal EMS but never strictly studied them in future work.

TABLE II: The modeling errors explored in study 2.

Vehicle Parameter	Coeff. of Drag	Frontal Area (m^2)	Mass Change (kg)	Coeff. of Rolling Resist.	Average Veh. Power Difference
Expected	0.259	2.6005	0	0.008	0%
Higher Mass	0.259	2.6005	+825	0.008	-26.2%
Lower Mass	0.259	2.6005	-825	0.008	26.6%
Higher Drag	0.3885	3.6005	0	0.008	-51.8%
Lower Drag	0.1295	1.6005	0	0.008	33.7%
Higher Rolling Resistance	0.259	2.6005	0	0.0016	-53.1%
Lower Rolling Resistance	0.259	2.6005	0	0.004	26.5%

2) Model Validation

Autonomie is a physics based vehicle FE model that has been demonstrated to show excellent correlation between real world operation of a 2010 Toyota Prius and a simulated 2010 Toyota Prius [38]. But, since the model of a 2010 Prius is not publicly available, the model of a 2010 Toyota Prius must be created by modifying the generic power split HEV model that comes preloaded in Autonomie. To update the generic power split HEV model to a 2010 Toyota Prius, the parameters shown in table I were modified. Note that the BSFC map was created by matching values to data from the 2010 Toyota Prius in the public domain [32].

To validate the 2010 Toyota Prius Autonomie model, the resulting FE numbers were compared to the real world measured FE numbers from Argonne National Labs [39] over the three standard U.S. Environmental Protection Agency drive cycles as shown in table III. Because the FE for each of the three drive cycles has less than 1.5% difference, the model was considered to be validated for further FE investigations.

This validated model of a 2010 Toyota Prius provides the Baseline EMS which will be contrasted with various applications of an Optimal EMS in the results section.

TABLE III: A comparison of the model simulated FE and physically measured FE for standard EPA drive cycles.

EPA Drive Cycle	Simulated Fuel Economy	Measured Fuel Economy[39]	Percent Difference
UDDS	75.4 mpg	75.6 mpg	0.3%
US06	45.9 mpg	45.3 mpg	-1.4%
HWFET	70.4 mpg	69.9 mpg	-0.7%

C. Optimal Energy Management Derivation

Derivation of an optimal solution requires numerous iterations which is computationally costly for a model as detailed as Autonomie. Therefore, to derive the Optimal EMS, a simplified equation based power split model must be used. But, once the Optimal EMS has been calculated, it can be incorporated into Autonomie as an override of the "engine power demand" and "engine on" model parameters. A schematic of the context for optimal control derivation is shown in figure 4.

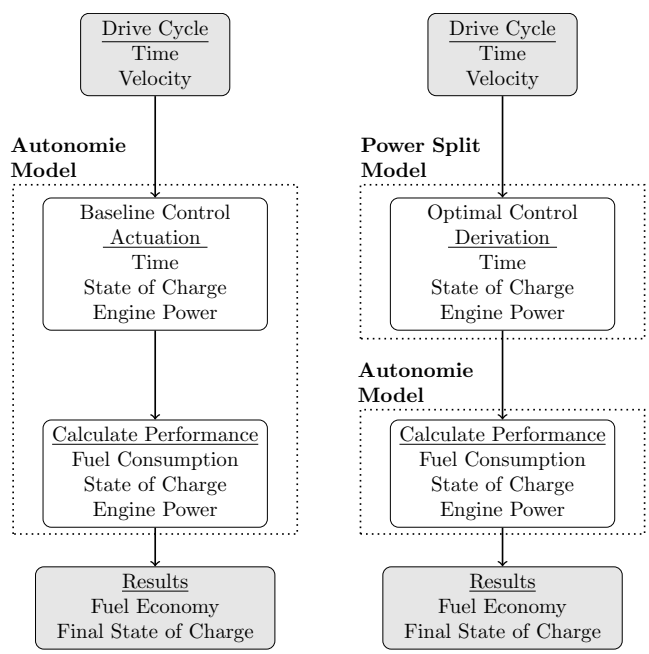

(a) Baseline EMS simulation (b) Optimal EMS simulation

Fig. 4: Comparison of the simulations defined as Baseline EMS (a) and Optimal EMS (b).

1) Dynamic Programming Optimization Justification

Prediction errors in general have not been rigorously studied but prediction error applied to a globally Optimal EMS has not been studied at all. As mentioned in the introduction, of the five studies that address prediction error [25]–[29], none use a globally Optimal EMS to investigate specific types of driving-derived prediction error over a full drive cycle. The study of prediction error on a globally Optimal EMS is required because it establishes the FE difference from the absolute optimal FE. If it can be shown that driving-derived prediction error does not degrade FE from a globally Optimal EMS,

then development of any non globally Optimal EMS would be unnecessary.

DP provides a convenient method of evaluating mispredictions because, as a by-product of solution computation, it creates the globally optimal solution for all evaluated state variables while ensuring the constraints are met. This solution by-product is an optimal control matrix which serves as a lookup table to generate near optimal solutions for all feasible states of the chosen state variables. For mispredictions where the state variables are at new values, the optimal control matrix still produces a near optimal control. DP provides a unique ability to understand and quantify the FE results from prediction errors and it is well understood by other researchers.

2) Dynamic Programming Formulation

DP finds the optimal solution using backwards recursion, which avoids solutions that are not optimal as defined by the Bellman principle of optimality [40], [41]. For every feasible state variable value, the optimal solution is stored. An appropriate DP scheme consists of a dynamic equation, a cost function, and state and control variable feasibility constraints

$$S(k+1) = S(k) + f(S, u, w, k)\Delta t \tag{2}$$

$$J = \sum_{k=0}^{N-1} f(S, u, w, k, \Delta t) \tag{3}$$

$$S_{\text{min}}(k) \leq S(k) \leq S_{\text{max}}(k) \qquad (k = 0, ...N) \tag{4}$$
$$u_{\text{min}}(k) \leq u(k) \leq u_{\text{max}}(k) \qquad (k = 0, ...N-1) \tag{5}$$

where S is the state, u is the control, w is the exogenous input, k is the timestep number, Δt is the timestep value, J is the cost, and N is the final timestep number.

For an HEV Optimal EMS derivation, the state is chosen to be the state of charge (SOC), the control is chosen to be the engine power, (P_{ICE}), the exogenous input is the vehicle velocity (v), and the cost is chosen to be the fuel mass required (m_{fuel}). This formulation with the added feasibility constraints for a 2010 Toyota Prius yields the following modified equations

$$\text{SOC}(k+1) = \text{SOC}(k) + f(\text{SOC}, P_{\text{ICE}}, v, k)\Delta t \tag{6}$$

$$\text{Cost} = \sum_{k=0}^{N-1} m_{\text{fuel}} \tag{7}$$

$$\text{SOC}_{\text{min}} \leq \text{SOC}(k) \leq \text{SOC}_{\text{max}} \qquad (k = 0, ...N) \tag{8}$$
$$P_{\text{ICE,min}} \leq P_{\text{ICE}}(k) \leq P_{\text{ICE,max}} \qquad (k = 0, ...N-1) \tag{9}$$

This HEV Optimal EMS derivation can then be tailored to a 2010 Toyota Prius by deriving a power-split model.

3) 2010 Toyota Prius Power-Split Model

The dynamic equation is derived using equations from the literature that describe a Toyota Hybrid System II [42], [43] and the parameters shown in table I. The total force on the vehicle, F_{vehicle}, is

$$F_{\text{vehicle}} = C_{rr}mg + \frac{1}{2}C_d\rho_{\text{air}}v(k)^2A_{\text{front}} + m\dot{v}(k) + mg\,\sin(\theta) \tag{10}$$

where C_{rr} is the coefficient of rolling resistance, m is the mass of the vehicle, g is the acceleration due to gravity $(9.81\ {}^{m}/_{sec^2})$, C_d is the coefficient of drag, ρ_{air} is the density of air $(1.1985\ {}^{kg}/_{m^3})$, v is the vehicle velocity, A_{front} is the frontal area, $\dot{v}$ is the vehicle acceleration (calculated using a numerical derivative), and θ is the elevation angle which is zero over the course of the drive cycle.

The power required by the vehicle, $P_{\text{vehicle}} = F_{\text{vehicle}}v(k)$, can come from either the engine or the battery, but excess engine power can also charge the battery. This can be expressed as

$$P_{\text{batt}} = F_{\text{vehicle}}v(k) - P_{\text{ICE}} \tag{11}$$

where P_{batt} is the battery power, P_{ICE} is the engine power. Note that when P_{batt} is negative, the battery is recharging.

The battery power shown in equation 11 does not account for the electric machine's efficiency. An overall efficiency map for a 2010 Toyota Prius is available in the literature [44] but the map changes as a function of voltage. It was found that incorporating a three dimensional interpolation function that would appropriately evaluate the efficiency maps was computationally prohibitive for the low level power-split model.

The change in the state of charge of the battery is given by $\frac{\text{d}}{\text{dt}}\text{SOC} = -{}^{I_{\text{batt}}}/_{Q_{\text{batt,o}}}$ where I_{batt} can be obtained by solving the quadratic electrical dynamic equation of the battery system of $P_{\text{batt}} = V_{\text{oc}}I_{\text{batt}} - R_{\text{int}}I_{\text{batt}}^2$ for the viable solution as $I_{\text{batt}} = \frac{V_{\text{oc}} - \sqrt{V_{\text{oc}}^2 - 4P_{\text{batt}}R_{\text{int}}}}{2R_{\text{int}}}$. Thus the change in state of charge of the battery is calculated as

$$\text{SOC}\,(k+1) = \text{SOC}\,(k) - \frac{V_{\text{oc}} - \sqrt{V_{\text{oc}}^2 - 4P_{\text{batt}}(k)R_{\text{int}}}}{2R_{\text{int}}Q_{\text{batt,o}}}\Delta t \tag{12}$$

where V_{oc} is the open circuit voltage, R_{int} is the internal resistance, and $Q_{\text{batt,o}}$ is the battery capacity.

Combining equations 10-12 produces the dynamic equation required in the DP algorithm

$$\text{SOC}\,(k+1) = \text{SOC}\,(k) - C_1 + C_2\sqrt{C_3 - C_4v(k) + C_5v(k)^3 + C_6\dot{v}(k)v(k) - C_7P_{\text{ICE}}} \tag{13}$$

where all C values are constants and are expressed as such for simplicity.

The cost function is derived by first obtaining a BSFC map through a cubic response surface [45] since a quadratic response surface would not match the structure of the BSFC

map available in the public domain [32]. A BSFC cubic response surface has the form of

$$\begin{aligned}\text{BSFC} = A_1 + A_2\omega_{\text{ICE}} + A_3T_{\text{ICE}} + \\ A_4\omega_{\text{ICE}}T_{\text{ICE}} + A_5\omega_{\text{ICE}}^2 + A_6T_{\text{ICE}}^2 + \\ A_7\omega_{\text{ICE}}T_{\text{ICE}}^2 + A_8\omega_{\text{ICE}}^2T_{\text{ICE}} + A_9T_{\text{ICE}}^3\end{aligned} \quad (14)$$

where all A values are constants, ω_{ICE} is the engine speed, and T_{ICE} is the engine torque. The surface developed is shown in figure 5. Once the BSFC response surface was developed, an ideal operating line can be computed that shows the minimum fuel consumption for any desired power (also shown in figure 5).

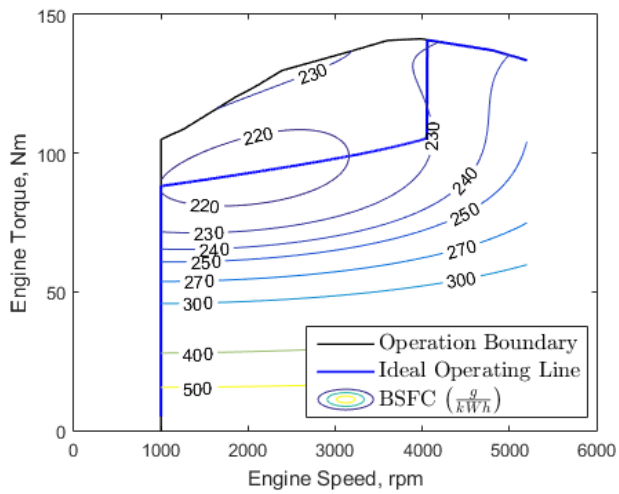

Fig. 5: The approximated BSFC map response surface created.

For a specified power and desired minimal fuel consumption, the associated engine speed, engine torque, and fuel rate is fixed which is the concept of the ideal operating line discussed in the introduction. This idea is expressed by the following equation

$$\omega_{\text{ICE}} = f\left(P_{\text{ICE}}\right) \quad (15)$$
$$T_{\text{ICE}} = f\left(P_{\text{ICE}}\right) \quad (16)$$
$$m_{\text{fuel}} = f\left(P_{\text{ICE}}\right) \quad (17)$$

The functions in equation 17 could be expressed as an analytical function fit, but since DP uses discrete time, expression as a look up table is sufficient.

Note that it is not required to limit solutions to exist only along the ideal operating line; it is possible that overall system loss could be lessened by straying from the ideal operating line. Several test cases were completed which allow straying from the ideal operating line, but the solution for the Optimal EMS derived in the low level power-split model always ended up on the ideal operating line anyway. Significant computational savings were achieved by then only considering solutions along the ideal operating line.

A dynamic final state of charge value penalty function of

$$\text{Penalty} = W\left(\text{SOC}_f - S(N)\right)^2; \quad (18)$$

is also required where W is an arbitrary weight value which was selected to be 100,000 and SOC_f=SOC_i=50%.

The cost is then expressed as

$$\text{Cost} = \sum_{k=0}^{N-1} f\left(P_{\text{ICE}}\right) + W\left(\text{SOC}_f - S(N)\right)^2 \quad (19)$$

Lastly, feasibility constraints must be incorporated into the model such as maximum ring gear speed, battery power, generator electric motor torque, generator electric motor speed, and generator electric motor power. It was found that the most limiting constraint was the generator electric motor speed which must be added to the DP formulation. The other constraints were incorporated in this research but are not shown due to their minimal effect.

To derive the maximum generator electric motor speed constraint, the following gearing relationship can be used

$$\omega_{\text{ICE}} = \omega_{\text{generator}}\frac{\rho}{1+\rho} + \omega_{\text{ring}}\frac{1}{1+\rho} \quad (20)$$

where $\rho = \frac{N_{\text{sun}}}{N_{\text{ring}}}$, $N_{\text{teeth,generator}} = 30$, and $N_{\text{teeth,ring}} = 78$. The ring gear speed is based on the vehicle speed as

$$\omega_{\text{ring}} = \frac{r_{\text{final drive}}v(k)}{R_{\text{wheel}}} \quad (21)$$

where $r_{\text{final drive}}$ is the final drive ratio and R_{wheel} is the wheel radius.

The constraint is then be expressed as

$$C_8\left[f\left(P_{\text{ICE}}\right)\right] + C_9v(k) \leq C_10 \quad (22)$$

where all C values are constants.

Putting everything together, the dynamic programming formulation of the global EMS derivation for a 2010 Toyota Prius is

$$\begin{aligned}\text{SOC}\left(k+1\right) = \text{SOC}\left(k\right) - C_1 \\ + C_2\sqrt{C_3 - C_4v(k) + C_5v(k)^3 + C_6\dot{v}(k)v(k) - C_7P_{\text{ICE}}}\end{aligned} \quad (23)$$

$$\text{Cost} = \sum_{k=0}^{N-1} f\left(P_{\text{ICE}}\right) + W\left(\text{SOC}_f - \text{SOC}(N)\right) \quad (24)$$

$$40\ \% \leq \text{SOC}(k) \leq 80\ \% \quad (k = 0, ...N) \quad (25)$$
$$0\ \text{kW} \leq P_{\text{ICE}}(k) \leq 73\ \text{kW} \quad (k = 0, ...N-1) \quad (26)$$
$$C_8\left[f\left(P_{\text{ICE}}\right)\right] + C_9v(k) \leq C_10 \quad (27)$$

where the following timestep, state, and engine power discretization values were used

$$\Delta t = 1\ \text{sec} \quad (28)$$
$$\Delta\text{SOC} = 0.001\% \quad (29)$$
$$\Delta P_{\text{ICE}} = 0.1\ \text{kW} \quad (30)$$

4) Optimal Control Model Validation

To validate this process, the Baseline EMS and the derived Optimal EMS were compared for three EPA cycles. The results are shown in table IV. The percent improvement numbers were calculated as

$$\text{Percent Improvement} = \frac{\text{Optimal FE} - \text{Baseline FE}}{\text{Baseline FE}} \tag{31}$$

where the FE is adjusted for differing SOC_f values according to the SAE J1911 "Recommended Practice for Measuring the Exhaust Emissions and FE of Hybrid-Electric Vehicles, Including Plug-in Hybrid Vehicles" standard [46].

Since there is a significant improvement in FE using the optimal control strategy implemented in Autonomie, the optimal control derivation technique is considered validated for further FE investigations. Globally Optimal EMS have been applied to these standard EPA cycles by numerous other researchers and the results in table IV can also serve as validation for future researchers.

TABLE IV: A comparison of the baseline control FE and DP derived optimal control FE over three EPA drive cycles.

EPA Drive Cycle	Baseline Control Fuel Economy	Optimal Control Fuel Economy	Percent Improvement
UDDS	75.4 mpg	83.2 mpg	10.4%
US06	45.9 mpg	48.9 mpg	6.5%
HWFET	70.4 mpg	72.6 mpg	3.1%

5) Optimal Control with Mispredictions

A key aspect of this research is the evaluation of mispredictions using DP derived optimal control. DP provides an optimal control solution matrix which is valid for any state of charge and time during the drive cycle. The optimal control solution matrix for the expected drive cycle (shown in figure 1b) was computed and is shown in figure 6. This matrix is used to evaluate all the mispredictions from study 1 and study 2. As a basis for comparison, the solution using the optimal control matrix for perfect prediction for each case was also computed.

Drive cycle mispredictions are handled by converting the time state variable to a distance state variable numerically as distance $= \sum_{k=0}^{N} v(k)$ since all mispredictions occur over the same route. The mean absolute percent error (MAPE) applied to vehicle velocity has been defined in other prediction error research [27] as

$$\text{MAPE} = \frac{1}{N}\sum_{k=0}^{N} \frac{|\text{Actual Velocity} - \text{Predicted Velocity}|}{\text{Actual Velocity}} \tag{32}$$

and is under 20% in almost misprediction cases studied. Examples of the mispredictions when the time state variable is converted to a distance state variable are shown in figure 7.

For any state not in the design space, the Baseline EMS is employed.

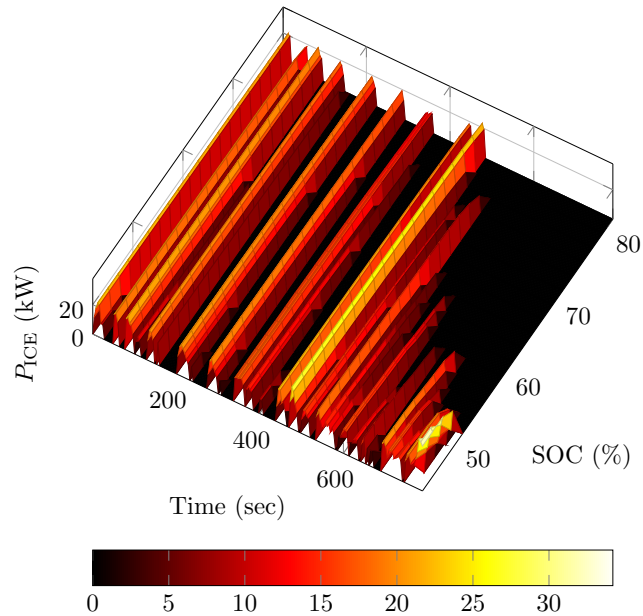

Fig. 6: The optimal control matrix derived using DP for the expected drive cycle.

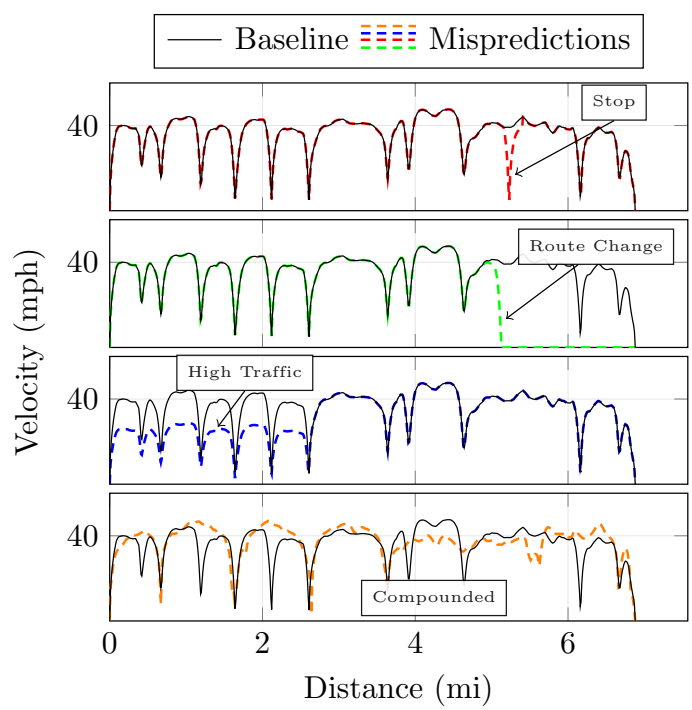

Fig. 7: Examples of the drive cycles when time is converted to a distance for the velocity prediction errors associated with study 1.

III. Results and Discussion

The results are organized into subsections for study 1 and study 2. For each type of misprediction, FE results are shown for perfect prediction and misprediction (prediction of the expected drive cycle or prediction of the expected vehicle parameters). A discussion of the results from each instance of misprediction are shown with the relevant vehicle signals.

Additional vehicle signals over each drive cycle are provided in the supplementary report.

A. Study 1: Optimal Energy Management Under Vehicle Velocity Mispredictions

FE was improved over the 2010 Toyota Prius Baseline EMS in every case except for under a fast route change and compounded misprediction drive cycles. The FE numbers from study 1 shown in figure 8 motivates the following five results about globally Optimal EMS: (1) exact drive cycle prediction increases FE as expected from the literature, (2) FE gains are maintained under mispredicted stops, (3) FE gains may not be maintained under route-change mispredictions, (4) FE gains are maintained under mispredicted traffic, and (5) FE gains may not be maintained under compounded mispredictions.

1) Result 1: Exact Prediction Increases Fuel Economy

Figure 8 shows a 10.9% increase in FE if the exact drive cycle is predicted. This increase in FE over the Baseline EMS comes from four sources:

1) Elimination of low power engine operation (fig 9a)
2) Reduction of high power engine operation (fig 9b)
3) Reduction of battery charging at the beginning of the drive cycle (fig 10a and 10b)
4) Increase in battery charging at the end of the drive cycle (fig 10a and 10b)

The elimination of low power engine operation and the reduction of high speed engine operation allows the engine to operate in a region on the brake specific fuel consumption map that has high efficiency, as shown in figure 9c. The Optimal EMS demonstrates the behavior shown in figures 9a and 9b over the entire drive cycle while maintaining the desired final state of charge and accumulates small decreases in fuel consumption which accumulate into a significant improvement in FE.

The Optimal EMS increases FE through a reduction of battery charging at the beginning of the drive cycle and an increase in battery charging at the end of the drive cycle. This is accomplished through lowered peak engine power (closer to an optimal value) during the approximate first half of the drive cycle and increased peak engine power (closer to an optimal value) during the approximate second half of the drive cycle. Both of these engine power modifications result in an increase in engine efficiency as shown on the brake specific fuel consumption map in figure 9c.

2) Result 2: Fuel Economy Gains are Maintained Under Stop Misprediction

Related to the Baseline EMS, figure 8 shows a +10.8% (out of +10.9% possible) increase in FE if one stop is mispredicted, a +7.9% (out of +10.7% possible) increase in FE if two stops are mispredicted, and a +5.1% (out of +11.2% possible) increase in FE if three stops are mispredicted. This demonstrates that FE gains through the Optimal EMS are maintained under stop mispredictions because a FE increase is still achieved in every misprediction case that was studied.

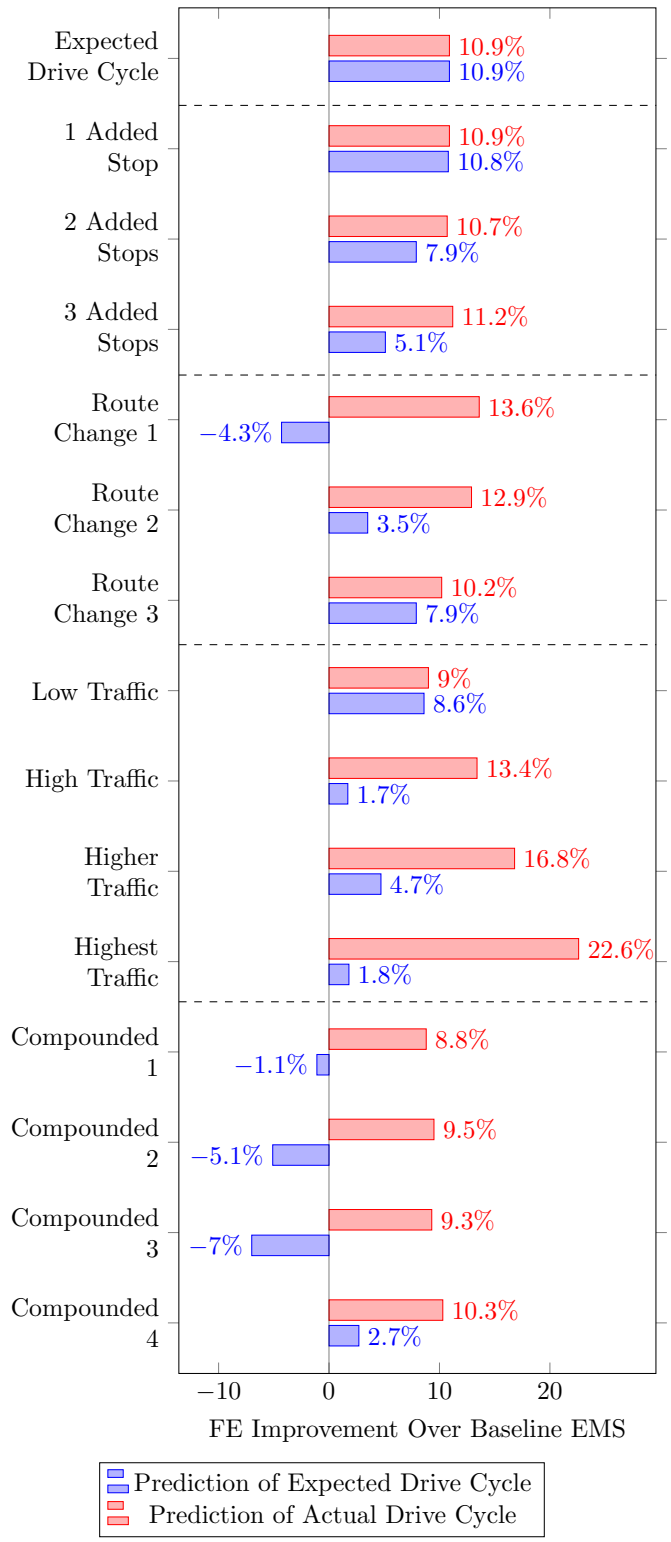

Fig. 8: FE results that compare Optimal EMS using incorrect and correct drive cycle predictions (drive cycles shown in figure 2).

Figure 11 shows the details of the "1 Added Stop" misprediction case. The actual and expected drive cycle differences are shown in figure 11b. When the stop is mispredicted, the Optimal EMS misapplies engine power as shown in figure

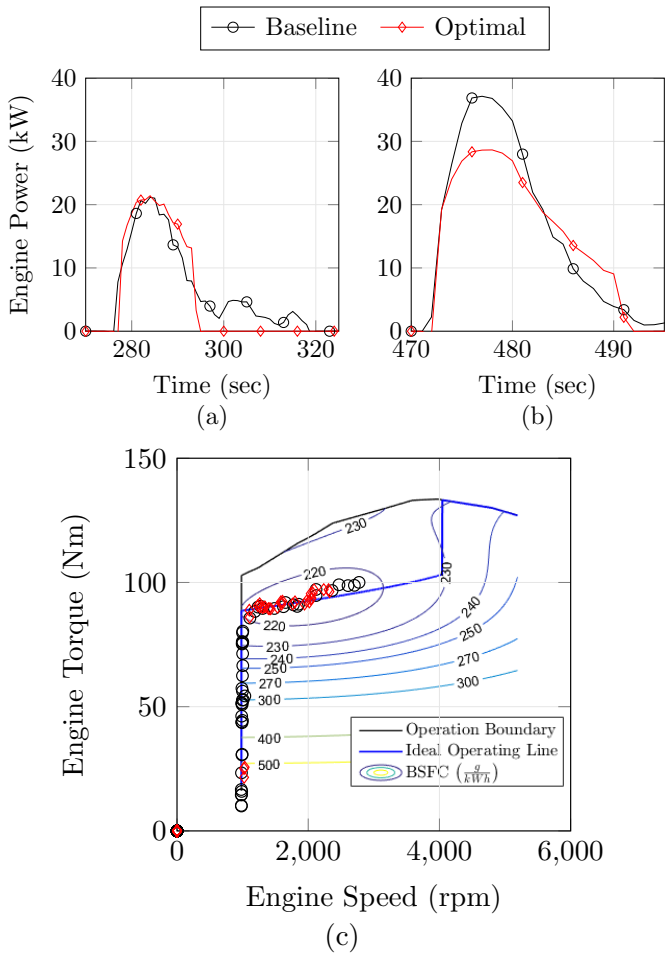

Fig. 9: Low engine speed operation (a), high engine speed operation (b), and engine brake specific fuel consumption (BSFC) comparisons (c).

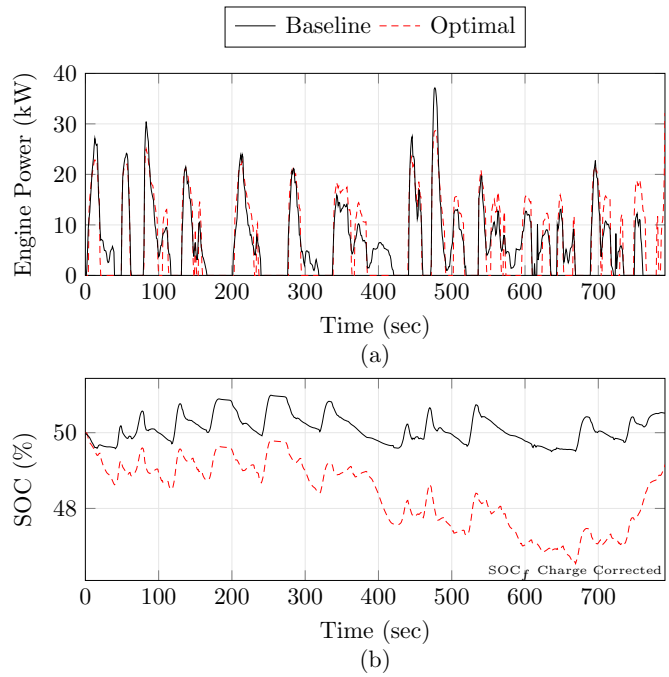

Fig. 10: Comparison of Baseline EMS and Optimal EMS engine operation and state of charge results for the expected drive cycle.

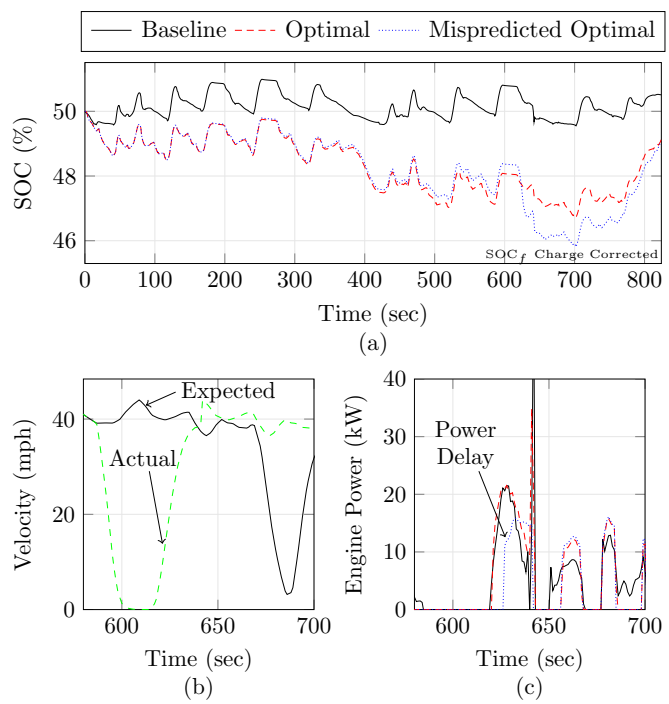

Fig. 11: Baseline, optimal control, and mispredicted optimal control results for the "1 Added Stop" misprediction case.

11c. This misapplication of engine power occurs because the Optimal EMS was derived assuming that the vehicle is traveling at 40 mph but the vehicle actually stops, remains stationary, and then accelerates. Overall, the engine power misapplication is a slight delay and does not affect fuel economy and state of charge significantly as shown in figures 8 and 11c.

3) Result 3: Fuel Economy Gains May be Lost from Route Change Misprediction

Related to the Baseline EMS, figure 8 shows a -4.3% (out of +13.6% possible) FE result if the drive cycle is the same as expected but then is suddenly ended shortly after it has begun (Route Change 1). This figure also shows a +3.5% (out of +12.9% possible) increase in FE if the drive cycle is suddenly ended midway through the predicted drive cycle, and a +7.9% (out of +10.2% possible) increase in FE if the drive cycle is suddenly ended most of the way through the predicted drive cycle. This demonstrates that FE increases through the Optimal EMS may be decreased when a route change is mispredicted.

The Optimal EMS seeks to equate the state of charge at the beginning and the end of the drive cycle only. During the drive cycle, the optimization routine is only constrained by the physical maximum and minimum battery charge limitations. Therefore, when a route change is mispredicted, the battery state of charge could be excessively high or low which could result in a loss of battery state of charge adjusted FE. This

battery state of charge discrepancy is shown in figure 12a, which presents results for "Route Change 1". Additionally, as can be seen in figure 12b, the mispredicted optimal control case seeks engine operation in anticipation of a forthcoming acceleration shown in figure 12a. But, since the acceleration shown in figure 12a is not realized, the FE is decreased.

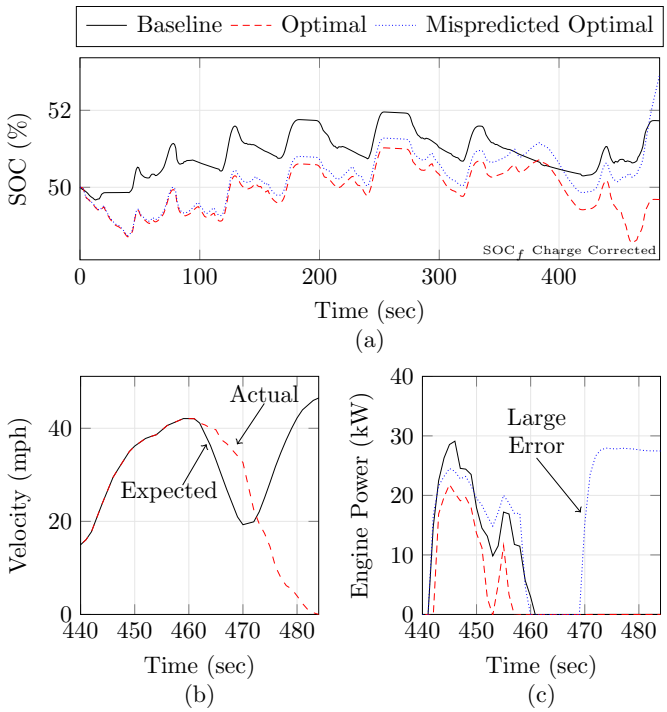

Fig. 12: Baseline, optimal control, and mispredicted optimal control results for the "Route Change 1' misprediction case.

4) Result 4: Fuel Economy Gains are Maintained Under Traffic Misprediction

Related to the Baseline EMS, figure 8 shows an +8.6% (out of +9.0% possible) increase in FE if traffic levels are lower than expected (higher than expected vehicle speeds), a +1.7% (out of +13.4% possible) increase in FE if traffic is higher than expected (low vehicle speed), a +4.7% (out of +16.8% possible) increase in FE if traffic is significantly higher than expected (lower vehicle speed), and +1.8% (out of +22.6% possible) increase in FE if traffic is much higher than expected (lowest vehicle speed). This demonstrates that the fuel economy gains from the Optimal EMS are maintained under traffic mispredictions because a FE increase is still achieved in every misprediction case with the caveat that if traffic is higher than predicted, there is a significant loss in *potential* FE improvements through the Optimal EMS.

For the "High Traffic" misprediction, the actual drive cycle is at speeds much lower than the predicted drive cycle as shown in figure 13b. This speed discrepancy results in the mispredicted Optimal EMS operating the engine at an excessively high power as shown in figure 13c. The higher than required engine power drives the battery state of charge up as shown in figure 13a. The Optimal EMS is still designed to end the state of charge at 50% so the state of charge is decreased over the second half of the drive cycle and a fuel economy improvement over the Baseline EMS is maintained.

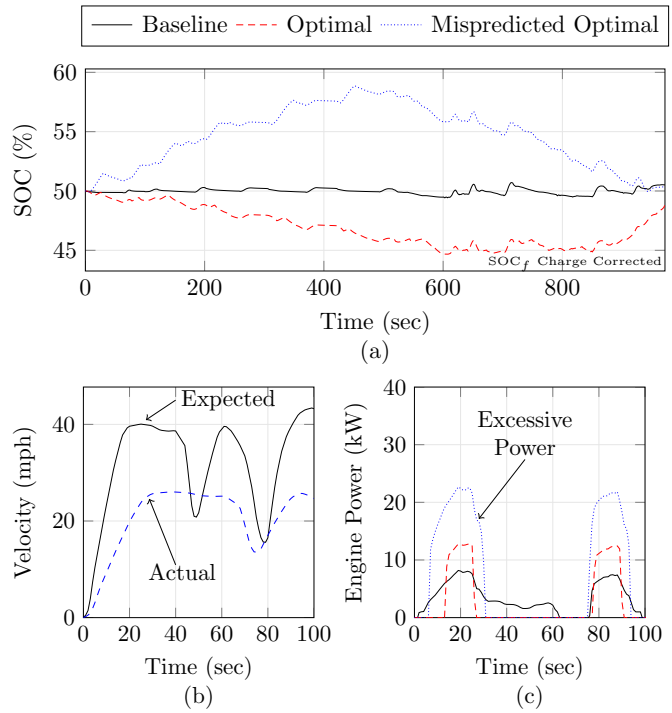

Fig. 13: Baseline vs optimal control results for the "High Traffic" misprediction case.

5) Result 5: Fuel Economy Gains May be Lost from Compound Prediction Errors

A real world driven alternate drive cycle along the same route produces mispredicted stops, traffic, and potentially route changes. Figure 8 shows a -1.1% (out of +8.8% possible) FE result for an alternate drive cycle driven along the same route, a -5.1% (out of +9.5% possible) FE result for another alternate drive cycle driven along the same route, a -7.0% (out of +9.3% possible) FE result for an alternate drive cycle driven that includes a wrong turn but was intended to be driven along the same route, and a +2.7% (out of +10.3% possible) FE result for a fourth alternate drive cycle driven along the same route.

Despite the conversion of the time state variable to a distance state variable, the velocities are significantly different along the entire drive cycle as shown in figure 7. The sections with the most drastic velocity discrepancies as shown in figure 14b result in sections of high power engine operation at completely inappropriate points in the drive cycle as shown in figure 14c. Because of these large discrepancies in engine operation, the FE is worse than the Baseline EMS in almost every case of compounded prediction errors.

6) Study 1 Summary

The following results were obtained in study 1:

1) Fuel economy gains from the Optimal EMS are **maintained** under stop mispredictions
2) Fuel economy gains from the Optimal EMS are **maintained** under traffic mispredictions

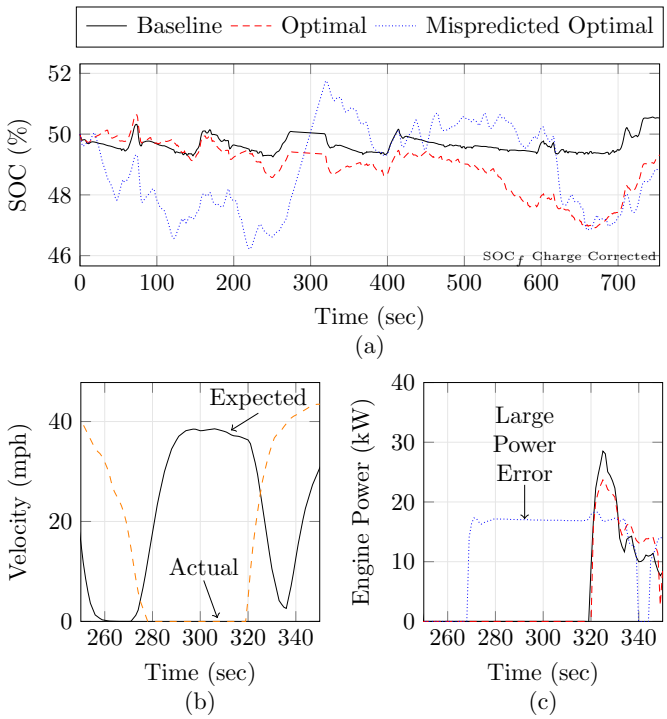

Fig. 14: Baseline vs optimal control results for the "Compounded 2" misprediction case.

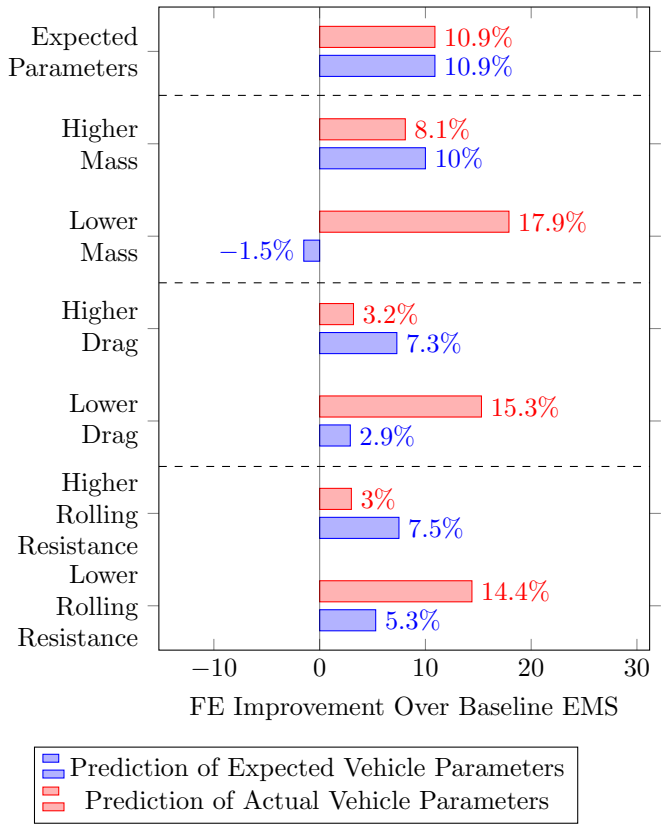

Fig. 15: FE results that compare Optimal EMS using incorrect and correct vehicle parameter prediction (vehicle parameters shown in table II).

3) Fuel economy gains from the Optimal EMS **may be lost** under route change mispredictions
4) Fuel economy gains from the Optimal EMS **may be lost** under compounded mispredictions

B. Study 2: Optimal Energy Management Vehicle Under Power Mispredictions

FE was improved over the 2010 Toyota Prius Baseline EMS in every type of power misprediction except when the vehicle mass is severely under predicted ("Lower Mass" case) which is unlikely to occur in standard vehicle operation. The FE numbers from study 2 shown in figure 15 motivate the following two results: (1) FE gains are maintained under higher than expected vehicle power mispredictions and (2) FE gains are maintained under lower than expected vehicle power mispredictions.

1) Result 6: Fuel Economy Gains are Maintained Under Higher than Predicted Vehicle Power

Related to the Baseline EMS, figure 15 shows an +10.0% (out of +8.1% possible) FE result for a higher than expected vehicle mass, a +7.3% (out of +3.2% possible) FE result for a higher than expected vehicle drag, and a +7.5% (out of +3.0% possible) FE result for a higher than expected rolling resistance.

When predicting vehicle power to be higher than actual vehicle power ("Higher Mass", "Higher Drag", and "Higher Rolling Resistance" cases), the Optimal EMS solution behaves in nearly the same as perfect prediction, except at a lower engine power, as seen in figure 16b. The result is a state of charge value well below 50% for the majority of the drive cycle as shown in figure 16a. The ending state of charge value is then significantly below the target value which results in a higher state of charge adjusted FE than the optimal solution based on the SAE J1711 standard [46].

2) Result 7: Fuel Economy Gains are Maintained Under Lower than Predicted Vehicle Power

Related to the Baseline EMS, figure 15 shows a -1.5% (out of +17.9% possible) FE result for a lower than expected vehicle mass, a +2.9% (out of +15.3% possible) FE result for a lower than expected vehicle drag, and a +5.3% (out of +14.4% possible) FE result for a lower than expected rolling resistance.

When predicting vehicle power to be lower than actual vehicle power ("Lower Mass", "Lower Drag", and "Lower Rolling Resistance" cases), the Optimal EMS solution behaves in nearly the same as perfect prediction, except at a higher peak value as seen in figure 17b. The result is a state of charge value well above 50% for the majority of the drive cycle as shown in figure 17a. The ending state of charge value is significantly above the target value which results in a lower state of charge adjusted FE than the optimal solution based on the SAE J1711 standard [46].

3) Study 2 Summary

The following results were obtained in study 2:

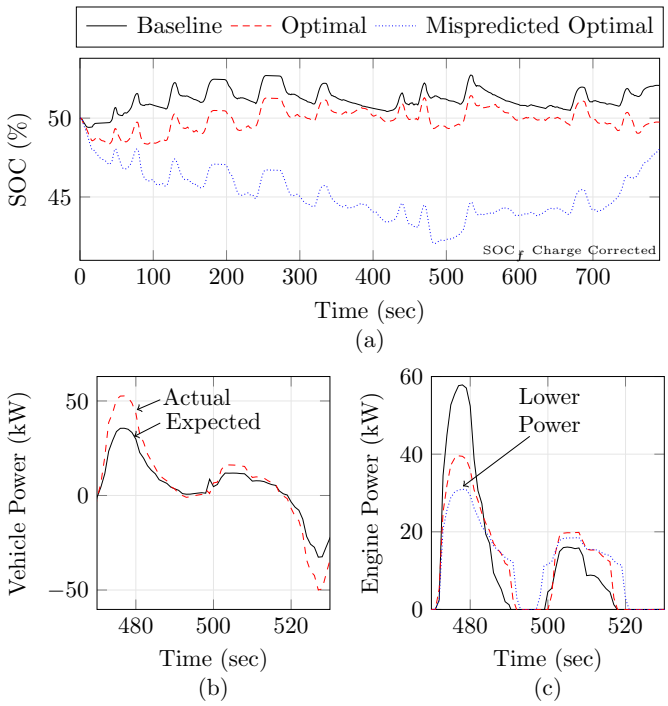

Fig. 16: Baseline vs optimal control results for the "Higher Mass" misprediction case.

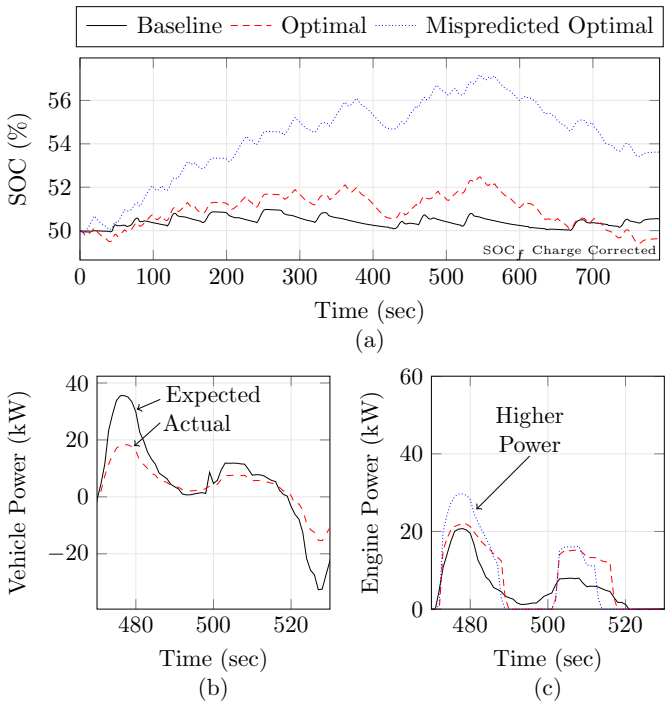

Fig. 17: Baseline vs optimal control results for the "Lower Mass" misprediction case.

1) Fuel economy gains from the Optimal EMS are **maintained** under vehicle parameter mispredictions
2) Vehicle parameter mispredictions that result in **lower** average vehicle power result in a **higher** operating battery state of charge
3) Vehicle parameter mispredictions that result in **higher** average vehicle power result in a **lower** operating battery state of charge

IV. Conclusions

In this study, an Optimal EMS with driving-derived mispredictions and vehicle power mispredictions was studied to quantify the fuel economy cost of misprediction. First, an expected drive cycle and fourteen drive cycle mispredictions were developed. Then, a validated 2010 Toyota Prius model was developed by updating the generic power-split HEV model in Autonomie with publicly available 2010 Toyota Prius data. Six cases of vehicle parameter mispredictions were also developed based on plausible values from the literature to investigate the effects of required vehicle power mispredictions. A globally Optimal EMS derivation was developed using DP and an equation based model for the Toyota Hybrid System II used by the Toyota Prius. A misprediction analysis technique was developed using the optimal control solution matrix from DP and converting the time variable to a distance variable.

For many of the driving-derived mispredictions (stops, traffic, and vehicle power), a fuel economy improvement of the Optimal EMS over the Baseline EMS is maintained. For compounded mispredictions and route change mispredictions the fuel economy gains from the Optimal EMS may be lost. The results from studies 1 and 2 suggest that FE improvements over the Baseline EMS through a globally Optimal EMS are possible without perfect prediction.

Evaluating driving-derived mispredictions puts any alternate EMS into a more realistic context. The techniques presented in this research can be applied to an alternate EMS such as Equivalent Consumption Minimization Strategy (ECMS), adaptive Equivalent Consumption Minimization Strategy (a-ECMS), Stochastic Dynamic Programming (SDP), or Model Predictive Control (MPC). But, an EMS designed to be stochastically robust such as a-ECMS or SDP, may not maintain a FE improvement when subjected to certain driving-derived mispredictions because driving-derived mispredictions (mispredicted stops, route change, etc.) are not stochastic. The results from this study indicate that a globally Optimal EMS may provide the best fuel economy improvements even when mispredictions exist.

Future work can consider the application of driving-derived mispredictions to other Optimal EMS from the literature, sensors/signals/algorithms required for vehicle operation prediction, and implementability of an Optimal EMS in a modern vehicle operating in the current driving environment. An initial study using only current vehicle speed and GPS location shows promising fuel economy results from an Optimal EMS [47].

Acknowledgment

The authors would like to thank Joshua Payne, Benjamin Geller, and Heraldo Stefanon of the Gasoline Hybrid Research Group at Toyota Motor Engineering & Manufacturing North America, Inc. in Ann Arbor, MI for their contributions and support.

REFERENCES

[1] R. Bishop, *Intelligent vehicle technology and trends*. trid.trb.org, 2005.

[2] O. Gusikhin, D. Filev, and N. Rychtyckyj, "Intelligent vehicle Systems:Applications and new trends," in *Informatics in Control Automation and Robotics*, ser. Lecture Notes Electrical Engineering, J. A. Cetto, J.-L. Ferrier, José Miguel Costa, and J. Filipe, Eds. Springer Berlin Heidelberg, 2008, pp. 3–14.

[3] Z. D. Asher, V. Wifvat, A. Navarro, S. Samuelsen, and T. Bradley, "The importance of HEV fuel economy and two research gaps preventing real world implementation of optimal energy management," in *SAE Technical Paper Series*, ser. SAE Technical Paper Series, vol. 1. 400 Commonwealth Drive, Warrendale, PA, United States: SAE International, 10 Jan. 2017.

[4] S. M. Lukic and A. Emadi, "Effects of drivetrain hybridization on fuel economy and dynamic performance of parallel hybrid electric vehicles," *IEEE Trans. Veh. Technol.*, vol. 53, no. 2, pp. 385–389, Mar. 2004.

[5] International Energy Agency, *Key World Energy Statistics 2016*. International Energy Agency, 2015.

[6] D. L. Greene and S. Ahmad, *Costs of US oil dependence: 2005 update*. United States. Department of Energy, 2005.

[7] M. van Moerkerk and W. Crijns-Graus, "A comparison of oil supply risks in EU, US, japan, china and india under different climate scenarios," *Energy Policy*, vol. 88, pp. 148–158, 2016.

[8] International Energy Agency, "CO2 emissions from fuel combustion," Tech. Rep., 2016.

[9] ——, "World energy outlook special report: Energy and air pollution," Tech. Rep., 2016.

[10] W. H. Organization, *World Health Statistics 2016: Monitoring Health for the Sustainable Development Goals (SDGs)*. World Health Organization, 2016.

[11] A. E. Atabani, I. A. Badruddin, S. Mekhilef, and A. S. Silitonga, "A review on global fuel economy standards, labels and technologies in the transportation sector," *Renewable Sustainable Energy Rev.*, vol. 15, no. 9, pp. 4586–4610, Dec. 2011.

[12] A. A. Frank, "Control method and apparatus for internal combustion engine electric hybrid vehicles," Patent 6 054 844, 25 Apr., 2000.

[13] K. Muta, M. Yamazaki, and J. Tokieda, "Development of new-generation hybrid system THS II-Drastic improvement of power performance and fuel economy," *SAE Trans. J. Mater. Manuf.*, vol. 113, no. 3, pp. 182–192, 2004.

[14] Q. Wang and A. A. Frank, "Plug-in HEV with CVT: configuration, control, and its concurrent multi-objective optimization by evolutionary algorithm," *Int.J Automot. Technol.*, vol. 15, no. 1, pp. 103–115, 1 Feb. 2014.

[15] A. Sciarretta, M. Back, and L. Guzzella, "Optimal control of parallel hybrid electric vehicles," *IEEE Trans. Control Syst. Technol.*, vol. 12, no. 3, pp. 352–363, May 2004.

[16] P. Zhang, F. Yan, and C. Du, "A comprehensive analysis of energy management strategies for hybrid electric vehicles based on bibliometrics," *Renewable Sustainable Energy Rev.*, vol. 48, pp. 88–104, 2015.

[17] C.-C. Lin, J.-M. Kang, J. W. Grizzle, and H. Peng, "Energy management strategy for a parallel hybrid electric truck," in *Proceedings of the 2001 American Control Conference. (Cat. No.01CH37148)*, vol. 4. ieeexplore.ieee.org, 2001, pp. 2878–2883 vol.4.

[18] N. Kim, S. Cha, and H. Peng, "Optimal control of hybrid electric vehicles based on pontryagin's minimum principle," *IEEE Trans. Control Syst. Technol.*, vol. 19, no. 5, pp. 1279–1287, 2011.

[19] D. Bianchi, L. Rolando, L. Serrao, S. Onori, G. Rizzoni, N. Al-Khayat, T.-M. Hsieh, and P. Kang, "A Rule-Based strategy for a Series/Parallel hybrid electric vehicle: An approach based on dynamic programming," in *ASME 2010 Dynamic Systems and Control Conference*. American Society of Mechanical Engineers, 1 Jan. 2010, pp. 507–514.

[20] G. Paganelli, S. Delprat, T. M. Guerra, J. Rimaux, and J. J. Santin, "Equivalent consumption minimization strategy for parallel hybrid powertrains," in *Vehicular Technology Conference. IEEE 55th Vehicular Technology Conference. VTC Spring 2002 (Cat. No.02CH37367)*, vol. 4. ieeexplore.ieee.org, 2002, pp. 2076–2081 vol.4.

[21] H. A. Borhan, A. Vahidi, A. M. Phillips, M. L. Kuang, and I. V. Kolmanovsky, "Predictive energy management of a power-split hybrid electric vehicle," in *2009 American Control Conference*. ieeexplore.ieee.org, Jun. 2009, pp. 3970–3976.

[22] C.-C. Lin, H. Peng, and J. W. Grizzle, "A stochastic control strategy for hybrid electric vehicles," in *Proceedings of the 2004 American Control Conference*, vol. 5. ieeexplore.ieee.org, Jun. 2004, pp. 4710–4715 vol.5.

[23] S. Onori, L. Serrao, and G. Rizzoni, "Adaptive equivalent consumption minimization strategy for hybrid electric vehicles," in *ASME 2010 Dynamic Systems and Control Conference*. American Society of Mechanical Engineers, 1 Jan. 2010, pp. 499–505.

[24] C. Zhang and A. Vahidi, "Route preview in energy management of plug-in hybrid vehicles," *IEEE Trans. Control Syst. Technol.*, vol. 20, no. 2, pp. 546–553, Mar. 2012.

[25] M. P. O'Keefe and T. Markel, "Dynamic programming applied to investigate energy management strategies for a plug-in HEV," National Renewable Energy Laboratory Golden, Colorado, USA, Tech. Rep., 2006.

[26] L. Fu, Ü. Ö. zgüner, P. Tulpule, and V. Marano, "Real-time energy management and sensitivity study for hybrid electric vehicles," in *Proceedings of the 2011 American Control Conference*. ieeexplore.ieee.org, Jun. 2011, pp. 2113–2118.

[27] Y. He, M. Chowdhury, P. Pisu, and Y. Ma, "An energy optimization strategy for power-split drivetrain plug-in hybrid electric vehicles," *Transp. Res. Part C: Emerg. Technol.*, vol. 22, pp. 29–41, 2012.

[28] D. F. Opila, X. Wang, R. McGee, R. Brent Gillespie, J. A. Cook, and J. W. Grizzle, "Real-World robustness for hybrid vehicle optimal energy management strategies incorporating drivability metrics," *J. Dyn. Syst. Meas. Control*, vol. 136, no. 6, p. 061011, 1 Nov. 2014.

[29] M. A. M. Zulkefli and Z. Sun, "Real-Time powertrain optimization strategy for connected hybrid electrical vehicle," in *ASME 2016 Dynamic Systems and Control Conference*. .asmedigitalcollection.asme.org, 2016, pp. V002T20A006–V002T20A006.

[30] C. C. Chan, "The state of the art of electric, hybrid, and fuel cell vehicles," *Proc. IEEE*, vol. 95, no. 4, pp. 704–718, Apr. 2007.

[31] U. S. D. o. Energy, "2017 best and worst fuel economy vehicles," https://www.fueleconomy.gov/feg/best-worst.shtml, accessed: 2017-2-21.

[32] N. Kawamoto, K. Naiki, T. Kawai, T. Shikida, and M. Tomatsuri, "Development of new 1.8-liter engine for hybrid vehicles," SAE Technical Paper, Tech. Rep., 2009.

[33] *Toyota 2010 Prius Owners Manual*.

[34] A. S. White, "Twenty years of projects on vehicle aerodynamics," *Int. J. Mech. Eng. Educ.*, vol. 27, no. 1, pp. 71–87, 1999.

[35] W. Blythe, T. D. Day, and W. D. Grimes, "3-dimensional simulation of vehicle response to tire blow-outs," SAE Technical Paper, Tech. Rep., 1998.

[36] S. K. Clark, *Mechanics of Pneumatic Tires*. U.S. Government Printing Office, 1981.

[37] T. van Keulen, B. de Jager, A. Serrarens, and M. Steinbuch, "Optimal energy management in hybrid electric trucks using route information," *Oil & Gas Science and Technology – Revue de lInstitut Français du Pétrole*, vol. 65, no. 1, pp. 103–113, 1 Jan. 2010.

[38] N. Kim, A. Rousseau, and E. Rask, "Autonomie model validation with test data for 2010 toyota prius," SAE Technical Paper, Tech. Rep., 2012.

[39] Argonne National Lab, "Downloadable dynamometer database," 16 Apr. 2015, title of the publication associated with this dataset: Test Summary Sheet.

[40] D. P. Bertsekas, D. P. Bertsekas, D. P. Bertsekas, and D. P. Bertsekas, *Dynamic programming and optimal control*. Athena Scientific Belmont, MA, 1995, vol. 1.

[41] R. Bellman, "Dynamic programming and lagrange multipliers," *Proc. Natl. Acad. Sci. U. S. A.*, vol. 42, no. 10, pp. 767–769, Oct. 1956.

[42] J. P. Arata, III, "Simulation and control strategy development of power-split hybrid-electric vehicles," Ph.D. dissertation, Georgia Institute of Technology, 2011.

[43] R. Rajamani, *Vehicle Dynamics and Control*. Springer Science & Business Media, 21 Dec. 2011.

[44] E. Efficiency and R. Energy, "Evaluation of the 2010 toyota prius hybrid synergy drive system," 2011.

[45] R. F. Gunst, "Response surface methodology: Process and product optimization using designed experiments," *Technometrics*, vol. 38, no. 3, pp. 284–286, 1996.

[46] SAE International, "Recommended practice for measuring the exhaust emissions and fuel economy of Hybrid-Electric vehicles," Tech. Rep. J1711, 2002.

[47] D. Baker, Z. Asher, and T. Bradley, "Investigation of vehicle speed prediction from neural network fit of real world driving data for improved engine On/Off control of the EcoCAR3 hybrid camaro," SAE Technical Paper, Tech. Rep., 2017.

Zachary D. Asher graduated with a Bachelor of Science degree in Mechanical Engineering from Colorado State University in 2009, a Master of Science degree in Mechanical and Aerospace Engineering from the University of Colorado at Colorado Springs in 2012, and worked full time in engineering industry from 2009 to 2015. He is currently a Doctorate of Philosophy candidate in the Department of Mechanical Engineering at Colorado State University and his research interests include mathematical modeling for control and optimization of mechanical systems.

David A. Baker graduated with a Bachelor of Science degree in Applied Physics from the State University of New York at Geneseo in 2015 and is currently a Master of Science student in the Department of Mechanical Engineering at Colorado State University. He is the engineering manager of the Colorado State University EcoCAR 3 competition team. His research interests include vehicle speed prediction and supervisory hybrid powertrain controls development and testing.

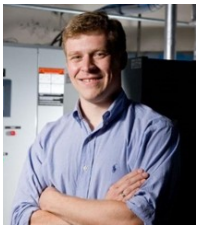

Thomas H. Bradley graduated with a Bachelor of Science degree in Mechanical Engineering from University of California at Davis in 2000, a Master of Science degree in Mechanical Engineering from the University of California at Davis in 2003, and a Doctorate of Philosophy degree in Mechanical Engineering: System Dynamics from the Georgia Institute of Technology in 2008. He is currently an Associate Professor in the Department of Mechanical Engineering and is the director of Systems Engineering at Colorado State University. Primary research interests include design of automotive, aerospace and energy systems, integrated controls and design optimization, and the validation of engineering design methods.